

Viscoelastic behaviour during the crystallisation of isotactic polypropylene

N. J. L. VAN RUTH

Faculty of Chemical Engineering, Technische Universiteit Eindhoven, Den Dolech 2, 5600 MB Eindhoven, The Netherlands

J. F. VEGA*

*Departamento de Física Macromolecular, Instituto de Estructura de la Materia, CSIC, Serrano 113 bis, 28006 Madrid, Spain
E-mail: imtv477@iem.cfmac.csic.es*

S. RASTOGI

Faculty of Chemical Engineering, Technische Universiteit Eindhoven, Den Dolech 2, 5600 MB Eindhoven, The Netherlands

J. MARTÍNEZ-SALAZAR

Departamento de Física Macromolecular, Instituto de Estructura de la Materia, CSIC, Serrano 113 bis, 28006 Madrid, Spain

Published online: 12 April 2006

Morphology and viscoelastic behaviour during the initial stages of crystallisation of isotactic polypropylene were explored as a function of time and angular frequency by light microscopy and dynamic oscillatory rheology. Results were evaluated according to the Krieger-Dougherty and Palierne models for viscoelastic suspensions of spheres. The data obtained from light microscopy were introduced in the rheological models reproducing quite well the viscoelastic response during crystallisation. The Palierne model was able to describe the behaviour of the system, though it was not possible to observe all the model's features due to a limited angular frequency range. Further, at high filler contents, an 'equilibrium' modulus needs to be introduced for the model to fit the experimental data. The exponent required to model the changes occurring in the 'equilibrium' modulus over time resembles that of chemical gelation more than physical gelation. © 2006 Springer Science + Business Media, Inc.

1. Introduction

The rheological behaviour of semi-crystalline polymers during crystallisation has not yet been well established due to its complexity and changes occurring over time. As the molten, amorphous polymer crystallises it generally forms spherulites, which results in an intermediate state of dispersed semi-crystalline spheres in an amorphous matrix. This intermediate state ceases to exist when the spherulites occupy the entire volume and all further crystallisation takes place within the spherulites. The duration of this intermediate state can differ greatly and is dependent on the kind of polymer and the crystallizing conditions.

At low crystalline content, when the spherulites are still growing and scarcely interact, the system can be

considered a suspension of solid particles in a viscoelastic matrix. Suspensions have been extensively modelled since Einstein's model [1] for dilute suspensions of solid particles in a Newtonian fluid, which was extended by others for suspensions of higher concentration, non-Newtonian fluids, and deformable particles. The Krieger and Dougherty model [2] describes the behaviour of systems of high particle concentration and can account for different particle size and shape. Palierne [3] developed a more general model, which considers particle size and nature, viscoelastic behaviour of the phases and hydrodynamic interactions. This model is able to account for increased values of the storage modulus G' at low frequencies, associated with relaxation mechanisms occurring in

*Author to whom all correspondence should be addressed.
0022-2461 © 2006 Springer Science + Business Media, Inc.
DOI: 10.1007/s10853-005-5507-6

the dispersed viscoelastic spherical particles, and interfacial tension between the phases.

The Palierne model was empirically modified by Bousmina and Muller [4] to take into account interactions between the spheres whereby a constant value G_e , also called the 'equilibrium' modulus, is added to the storage modulus G' to represent these interactions.

The polymer used here to explore rheological behaviour during crystallization is an isotactic polypropylene (iPP). The crystallisation behaviour of this polymer is well known and relatively easy to analyse due to relatively slow rates of crystallisation and spherulite growth and well-defined spherulite morphology.

This study was designed to determine whether the Palierne model can describe changing viscoelastic behaviour during crystallisation, and to explore its possible use in analysing changes in the volume fraction of the dispersed phase, or filler content, as a function of time. Filler content data from light microscopy were used to model the rheology of the crystallising polymer by using the Palierne and the Krieger and Dougherty, which, unlike the former, does not require knowledge of the viscoelastic properties of the dispersed phase.

2. Experimental

2.1. Material preparation

Isotactic polypropylene (iPP) grade, $M_w = 540$ kg/mol; $M_w/M_n = 4.4$; tacticity = 91.2% mmm, was supplied in granular form by Repsol-YPF, Spain. For the dynamic oscillatory experiments, the material was compression moulded into a 1.5 mm film on a hot-press at 200°C, at a nominal pressure of 150 bars. For the microscopy experiments, the iPP was compressed into a 40 μm film.

2.2. Dynamic oscillatory rheometry

A Bohlin CVO 120 dynamic mechanical thermal analyser with a 15 mm parallel plate measuring system was used for the oscillatory rheological determinations. Samples were cut from the film prepared by compression moulding. The samples were melted at 175°C for 3 min after which the gap between the plates was set at 750 μm . Higher temperatures and annealing times are necessary for a complete loss of memory in iPP [5]. However, this is not our main concern, but at least the same temperature history in rheological and microscopy experiments. This has been done in both experimental techniques, and then the same memory effects are expected.

Once trimmed and allowed to relax for 5 min at 175°C, the samples were cooled to the crystallisation temperatures tested (135 and 130°C) by manually lowering the temperature in steps (175°C \rightarrow 136°C \rightarrow 135°C and 175°C \rightarrow 135°C \rightarrow 132°C \rightarrow 130°C, respectively); the next temperature was set after reaching the previous temperature. The real temperature between the plates was measured by a platinum resistance probe. The steady state temperature in the range 120 to 140°C was found to be

2°C higher than that indicated by the equipment, corresponding to crystallisation temperatures of 137 and 132°C respectively. Real temperature fluctuations during manual cooling were also measured to reproduce the thermal history of the material as accurately as possible for the light microscopy experiments.

Time-sweeps were started as soon as the measurement temperature was reached at a frequency of 0.628 rad/s and a target strain of 0.02. All the crystallisation experiments were performed with gap control to stabilise the normal force.

During crystallisation, frequency sweeps were also performed at the defined time intervals: 1 min at 130°C and 5 min at 135°C. The experiment was run twice at each temperature, once in an upward sweep direction and once in a downward direction. Results were averaged to compensate for the effects of crystallisation during the sweep. The following frequencies were used: 62.8, 29.0, 13.4, 6.12, 2.81, 1.29, 0.594, 0.273, 0.126 rad/s at 135°C and 62.8, 29.5, 13.6, 6.28, 2.92, 1.36, 0.628 rad/s at 130°C. The times for each sweep were 120 s for measurements at 135°C and 30 s for those at 130°C. The first sweep was started immediately after the measurement temperature was reached, and thereafter sweeps were performed at the indicated intervals. Because of the averaging of the up and down sweep, half the measurement time (60 s for 135°C and 15 s for 130°C) was added to the starting time of each sweep, this time being valid for all frequencies in the sweep.

During the frequency sweep experiments, stress was set to vary proportionally with the square root of the frequency. The initial stress was set such that the strain was of the order 10^{-2} during the sweep, and was adjusted when crystallisation commenced. In any case the strain applied during measurements resulted always below 0.05. Additional tests (varying stress and strain levels) and literature results [6] have been shown this strain level does not affect quiescent crystallisation. In addition, throughout the tests a gap adjustment according to the tensile force transducer of the rheometer allowed the longitudinal stress induced by the size variation of the samples to be eliminated.

2.3. Light microscopy

A Nikon Eclipse polarizing microscope (E600POL) in cross-polarizing mode was used for the light microscopy experiments. Pictures were taken with a Nikon digital still camera (DXM1200). The spherulite growth rate was determined by crystallising the material on a Metler FT82 hot-stage following a similar thermal pattern to that observed in the rheometer. Images were obtained at defined times to evaluate spherulite changes in time. All the samples showed very homogeneous morphological features. A portion of the image was considered to describe well the whole sample in each case. Nuclei density has been obtained from these portions by counting, dividing by the area of the portion and converting into nuclei per volume unit.

3. Results and discussion

Fig. 1 shows the time sweeps performed to give an idea of the speed and rheological response of crystallisation at the temperatures chosen for subsequent experiments. A significant difference in crystallization speed was observed at the two temperatures tested. Moreover, both sweeps showed an early plateau indicating that crystallisation had not started before the measurements were taken.

Changes in spherulite radius over time are shown in Fig. 2. The radial growth rates of $0.083 \mu\text{m/s}$ at $T = 132^\circ\text{C}$ and $0.024 \mu\text{m/s}$ at $T = 137^\circ\text{C}$ can be used to calculate spherulite growth rate as a function of time. The latter in turn gives the filler content as a function of time at a given density of nuclei:

$$\phi_{\text{micr}} = (4/3 \cdot \pi \cdot R^3) \times N_{\text{nucl}} \quad (1)$$

N_{nucl} being the density of nuclei (μm^{-3}) and R the spherulite radius (μm).

Figs 3a–d are micrographs of the 132°C sample showing suspended spherulites at different times. Nucleus density in the microscopy experiment was $4.2 \cdot 10^{-6}$ nuclei per μm^3 at 132°C and $0.56 \cdot 10^{-6}$ nuclei per μm^3 at 137°C .

The following relations show how the rheological features zero shear viscosity, η_0 , and the experimental dynamic moduli, G' and G'' can be expressed as a function

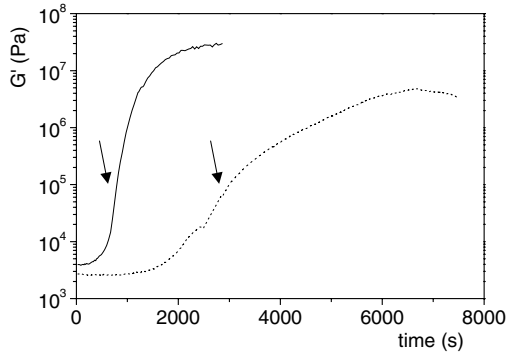


Figure 1 Time sweeps performed at 132°C (solid line) and 137°C (dashed line) at an angular frequency of 0.628 rad/s and target strain of 0.02 . The arrows indicates the time when the system is full of spherulites (from microscopy).

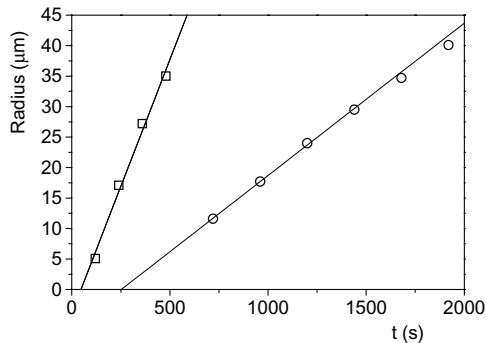


Figure 2 Change in spherulite radius over time at (\square) $T = 132^\circ\text{C}$ and (\circ) $T = 137^\circ\text{C}$.

of the filler content, i.e. the volume fraction of dispersed phase ϕ , allowing the quantification of the time dependence of viscoelastic properties.

Zero shear viscosity, η_0 , is given by the Cross fit to complex viscosity [7]:

$$|\eta^*| = \frac{\eta_0}{1 + (\tau_0 \omega)^n} \quad (2)$$

where τ_0 is a characteristic relaxation time and n an index that accounts for the frequency dependence of the complex viscosity. Similar models have been used to obtain these rheological parameters during crystallisation of iPP and polyethylene [8].

Figs 4a and b show the fits obtained and Table I lists the corresponding η_0 , τ_0 and n values. The model describes well the behaviour observed in the modulus of the complex viscosity function at short crystallisation times, as it is indicated by the solid lines in the figures. For these short times, a levelling off in the complex viscosity moduli at low frequencies is observed. For the highest crystallisation times, the experimental results indicate straight-line power law behaviour, indicated by the dotted lines, and then η_0 and τ_0 cannot be accurately determined. The data from the Cross-fit can then be introduced into the Krieger-Dougherty developed for suspensions [2]:

$$\eta = \eta_s \left(1 - \frac{\phi}{\phi_m}\right)^{-[\eta] \cdot \phi_m} \quad (3)$$

where η is the viscosity, η_s the viscosity of the suspending medium, ϕ the filler content, ϕ_m the maximum packing filler content and $[\eta]$ the intrinsic viscosity. This equation was, in principle, developed for steady shear viscosity with shear rate dependent values of ϕ_m and $[\eta]$ [2]. Al-Hadithi *et al.* pointed out that the magnitude of the viscosity in steady shear and in dynamic experiments could be different in heterogeneous systems [9]. However, it has been experimentally demonstrated that both physical properties are quite similar for iPP filled with solid particles up to filler content of around 40% [10]. This

TABLE I Numerical cross-fit results to the experimental data of the complex viscosity in Figs 4a and b

t (s)	$T = 132^\circ\text{C}$			$T = 137^\circ\text{C}$			
	η_0 ($10^3 \text{ Pa}\cdot\text{s}$)	τ_0 (s)	n	t (s)	η_0 ($10^3 \text{ Pa}\cdot\text{s}$)	τ_0 (s)	n
15/75	23.8	1.4	0.64	60	18.5	1.59	0.60
135	30.8	2.2	0.62	1260	18.5	1.59	0.60
195	33.3	1.9	0.64	1560	20.5	1.34	0.61
255	53.2	3.7	0.63	1860	26.4	1.97	0.62
315	76.8	4.5	0.63	2160	51.2	5.60	0.59
375	157.4	9.1	0.65	2460	294	70.0	0.60
435	n.d.	n.d.	0.67	2760	n.d.	n.d.	0.68
615	n.d.	n.d.	0.79	3060	n.d.	n.d.	0.80

Note. n.d. means not determined.

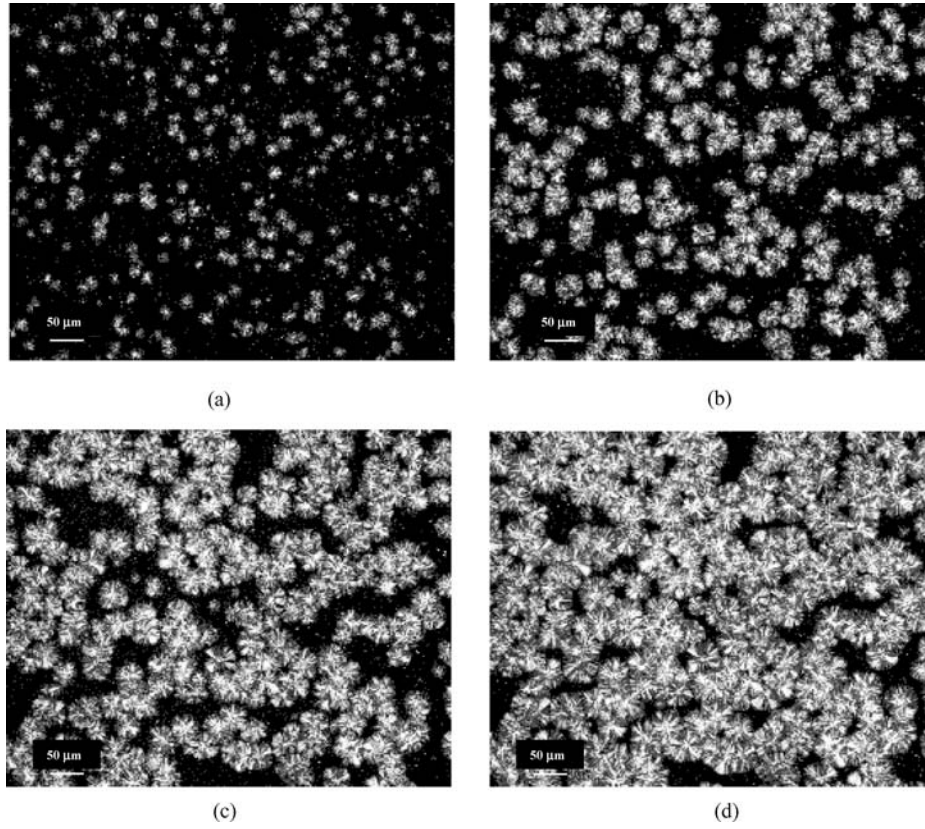


Figure 3 Micrographs showing crystallisation at $T = 132^{\circ}\text{C}$ at different times. Nucleus density is 4.2×10^{-6} nuclei per μm^3 . (a) $t = 240$ s. (b) $t = 360$ s. (c) $t = 480$ s. (d) $t = 600$ s.

experimental result allows us to argue that in crystallising polypropylene, considered as a filled system in the early stages of the crystallisation process, the steady-shear and dynamic complex viscosity are similar in magnitude as a first approximation. In other words, we do not expect strong differences for the zero shear viscosity values obtained from both types of experiments, due to the fact that at very low shear rates ($\dot{\gamma} \rightarrow 0$), i.e. in the linear viscoelastic region, the structure of these complex systems is hardly destroyed.

The spherulite growth rate and the nucleus density data obtained by light microscopy can be used to model the rheological results at the given temperature. This density remains constant during crystallisation. We have calculated the time evolution of the filler content, ϕ_{micr} (Equation 1), and then the Krieger-Dougherty equation can be tested for the values of η_0 and listed in Table I. In the model of Krieger-Dougherty given by Equation 3, the parameters ϕ_m and $[\eta]$ are strongly dependent on particle shape. A collection of values can be found in the literature for a number of suspensions with different type of particles [11–13]. We have considered that the spherulites behave as spherical particles. Thus the values of ϕ_m and $[\eta]$ are 0.61 and 3.28 respectively [13]. Fits for both temperatures are shown in Fig. 5. The agreement between microscopy modelled and experimental rheological results is very good.

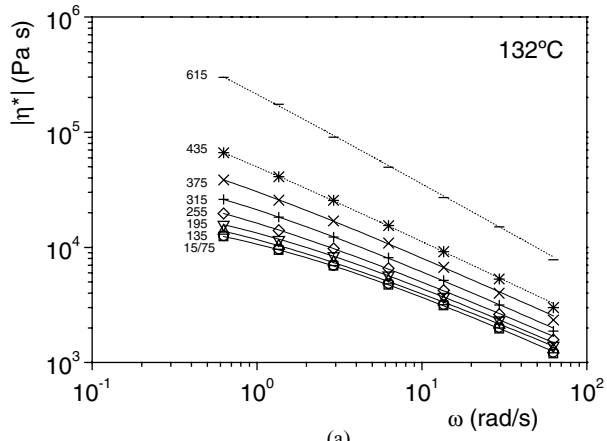
In the same way, the G' values in Figs 6a and b recorded during crystallisation can be fitted using the Palierne model for heterogeneous systems [3]:

$$G_b^* = G_m^* \frac{1 + 3\phi H}{1 - 2\phi H} \quad (4)$$

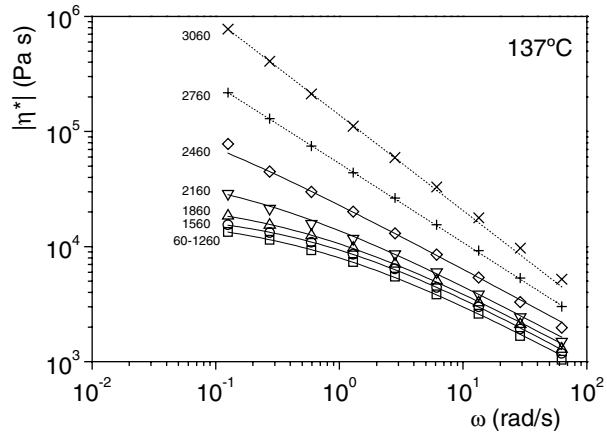
where H :

$$H = \frac{4(\alpha/R) \times (2G_m^* + 5G_d^*) + (G_d^* - G_m^*) \times (16G_m^* + 19G_d^*)}{40(\alpha/R) \times (G_m^* + G_d^*) + (2G_d^* + 3G_m^*) \times (16G_m^* + 19G_d^*)} \quad (5)$$

G_d^* being the modulus of the dispersed phase, G_m^* the modulus of the matrix, R the radius of the sphere, α the interfacial tension and ϕ the volume fraction of the dispersed phase obtained from light microscopy measurements, ϕ_{micr} (Equation 1). The modulus of the matrix (the amorphous phase) was taken as that shown at the beginning of the experiment, before the start of crystallisation. The modulus of the dispersed phase (the semicrystalline phase) was taken as that shown approximately at the time when the sample was completely filled with spherulites. The dispersed phase at this point is not an ideal crystalline phase but contains some non-marginal amorphous material. The G' values for the dispersed phase modulus



(a)



(b)

Figure 4 Results of the cross-fit for the modulus of complex viscosity at (a) $T = 132^\circ\text{C}$ and (b) $T = 137^\circ\text{C}$ and different crystallisation times.

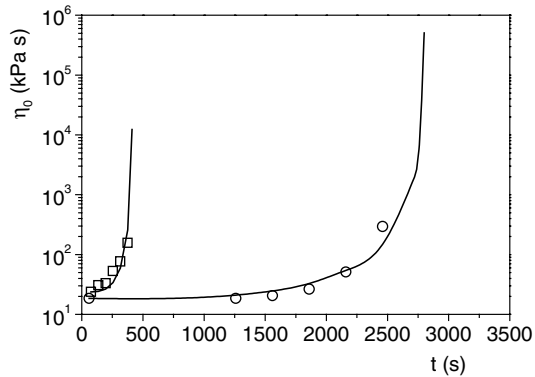
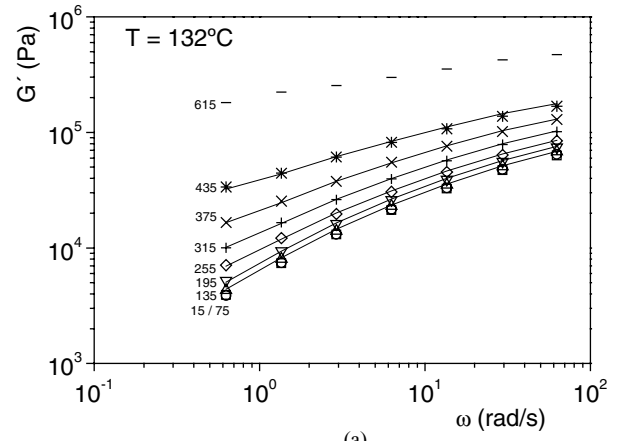
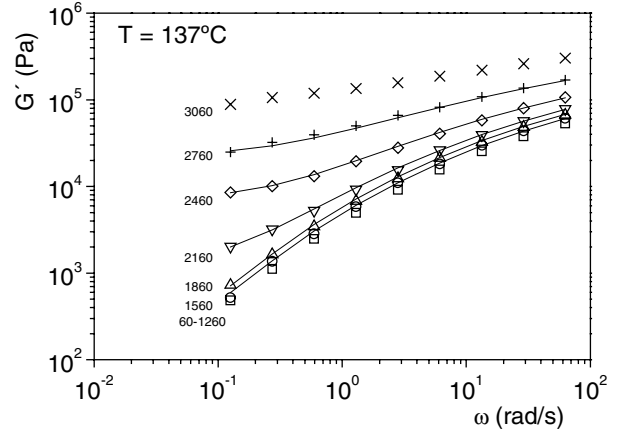


Figure 5 Time evolution of Newtonian viscosity during crystallisation at (□) 132°C and (○) 137°C . The lines are the calculated values using light microscopy results of ϕ_{micr} and the Krieger-Dougherty model (Equation 3).

chosen (non-fitted values at the top of Fig. 6) show power law behaviour for both temperatures, indicating the system has reached a solid-like behaviour. However, later in time the dispersed phase even evolves giving rise to a stronger increase in linear viscoelastic properties, as it is seen in Fig. 1. This means that at long times the properties of the dispersed phase are different from those at the early



(a)



(b)

Figure 6 Change in G' as a function of the time and angular frequency (time in seconds). Data appearing in the figure top (non-fitted) and bottom are the experimental results used in the Palieme model for the moduli of the dispersed phase and the matrix respectively: (a) 132°C and (b) 137°C .

stages of the crystallisation process, where the Palieme model has been applied.

The fits to Equations 4 and 5 for $T = 132^\circ\text{C}$ and $T = 137^\circ\text{C}$ are shown in Figs 6a,b, respectively. Unfortunately, because of the long measurement times, the range tested did not include sufficiently low frequencies to observe any possible effect of interfacial tension in the fitting procedure, thus the α/R ratio could not be computed. In any case, one would expect some changes in this value as crystallisation proceed (constant α and variable R). However, we have selected high values of α/R ($\alpha \rightarrow \infty$) to account for a sharp transition between the matrix (amorphous melt) and dispersed (semicrystalline solid) phases. Moreover, at high filler contents, an 'equilibrium' modulus, G_{eq} , has to be added to the Palieme model in Equations 4 and 5 to account for low angular frequency behaviour when calculating the storage modulus G' . The values of G_{eq} applied are provided in Table II. The modelling of G_{eq} obtained from the fitting of experimental results to phenomenological and mechanical models has been widely performed in the literature [4, 14, 15] to explain experimental low frequency behaviour. We are aware that the

TABLE II Values of the ‘equilibrium’ modulus used in the Palierne model in Figs 6a and b

$T = 132^{\circ}\text{C}$		$T = 137^{\circ}\text{C}$	
t (s)	G_{eq} (Pa)	t (s)	G_{eq} (Pa)
15/75	0	60	0
135	0	1260	0
195	0	1560	0
255	1100	1860	0
315	2600	2160	1150
375	6300	2460	7150
435	17300	2760	23150

value obtained here only from Palierne fit comes from a fitting procedure, but some testing can be performed in order to compare the results obtained with those from other works. The values of the “equilibrium” modulus in Table II can be fitted by [16, 17]:

$$G_{\text{eq}} = k(\phi - \phi_0)^f \quad (6)$$

The values for ϕ_0 are those for which the ‘equilibrium’ modulus is still zero and were located at around 0.10–0.15. The values obtained for k and f in Equation 6 were 10^5 and 1.8, respectively. The results of the fit are shown in Fig 7. The values obtained for ϕ_0 are close to the predicted by the continuum percolation theory. Statistical percolation is an established theory, which is suitable for randomly dispersed but not interacting fillers. In three-dimensional systems, the theory predicts a percolation volume fraction of 0.16 to form a random network structure [17]. The values found for the exponent f can be compared to exponent values derived from gelation theories for storage modulus changes. A value for f of about 3.8 is expected for a physical gel [17]; values of 2–3 being quoted for chemical gels [18, 19]. Values corresponding to chemical gels of high molecular weight precursors have been reported in studies in which iPP crystallisation is considered a physical gelation mechanism [18].

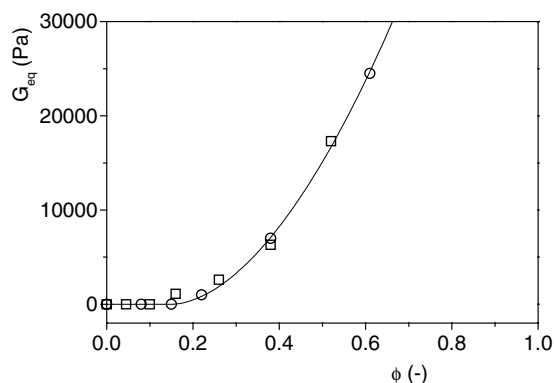


Figure 7 Change in the ‘equilibrium’ modulus as a function of filler content (time) at (\square) $T = 132^{\circ}\text{C}$ and (\circ) $T = 137^{\circ}\text{C}$. The line is the fit to Equation 6 with parameters: $K = 10^5$ Pa, $\phi_0 = 0.15$ and $f = 1.8$.

4. Conclusions

Filler content obtained from light microscopy explains rheological results expressed in terms of the Krieger-Dougherty and the Palierne models for heterogeneous systems. For the latter case this is an indication that the modulus selected for the dispersed phase was close to reality, and thus very different to the modulus corresponding to the actual polypropylene when crystallised to its normal extent. It was also shown that the system could be described as one of dispersed spheres in a matrix, for which the Palierne model is designed. The Palierne model offers a good description of viscoelastic behaviour during crystallisation in the frequency window tested, though behaviour at low frequencies could not be established. The explanation for the use of the ‘equilibrium’ modulus to model the low frequency behaviour lies in touching of the spherulites. The values found for the exponent of the increase in ‘equilibrium’ modulus with time corresponded more to values reported for chemical than physical gelation.

To further investigate the validity of the Palierne model for this type of system, experiments at lower angular frequencies should serve to determine whether the Palierne model is also capable of describing behaviour when changing spherulite radius and interfacial energy affect the data provided by the model. The application of novel experimental procedures to “freeze” the morphology at given crystallisation extent can be very helpful to get a deeper understanding of the crystallisation process [20].

Acknowledgments

Thanks are due to the MCYT (Grant MAT2002-01242) for financial support.

References

1. A. EINSTEIN, *Ann. Phys.* **34** (1911) 591.
2. I. M. KRIEGER and T. J. DOUGHERTY, *Trans. Soc. Rheol.* **3** (1959) 137.
3. J. F. PALIERNE, *Rheol. Acta.* **29** (1990) 204.
4. M. BOUSMINA and R. MULLER, *J. Rheol.* **37** (1993) 663.
5. G. C. ALFONSO and A. ZIABICKI, *Coll. and Polym. Sci.* **273** (1995) 317.
6. F. H. M. SWARTJES, “Stress Induced Crystallisation in Elongational Flow” (Ph.D. Thesis, Eindhoven University of Technology, The Netherlands, 2001).
7. R. B. BIRD, R. ARMSTRONG and O. HASSAGER, “Dynamics of Polymer Liquids” (John Wiley and Sons, New York, 1987).
8. K. BOUTAHAR, C. CARROT and J. GUILLET, *Macromolecules* **31** (1998) 1921.
9. T. S. R. AL-HADITHI, H. A. BARNES and K. WALTERS, *Coll. Polym. Sci.* **270** (1992) 40.
10. J. M. ADAMS and K. WALTERS, *Makromol. Chem., Macromol. Symp.* **68** (1993) 227.
11. B. CLARKE, *Trans. Inst. Chem. Eng.* **45** (1967) 251.
12. R. TURIAN and T.-F. YUAN, *AiChE J.* **23** (1977) 232.
13. H. GIESEKUS, “Physical Properties of Food” (Applied Science Publishers, London, 1983).
14. N. CASSON, “Rheology of Dispersed Systems” (Pergamon Press, London, 1959).

15. L. A. UTRACKI, "Rheological Measurements" (Hanser Publishers, Munich, 1989).
16. R. ZALLEN, "The Physics of Amorphous Solids" (Wiley, New York, 1983).
17. M. SAHIMI, "Applications of Percolation Theory" (Taylor and Francis, London, 1984).
18. M. ADAM, M. DELSANTI and D. DURAN, *Macromolecules* **18** (1985) 2285.
19. N. V. POGODINA and H. H. WINTER, *ibid.* **31** (1998) 8164.
20. A. ACIERNO and N. GRIZZUTI, *J. Rheol.* **47** (2003) 563.

*Received 7 June
and accepted 11 July 2005*